Bioorganic & Medicinal Chemistry Letters 21 (2011) 3148–3151

Contents lists available at ScienceDirect

Bioorganic & Medicinal Chemistry Letters

journal homepage: www.elsevier.com/locate/bmcl

Simultaneous DSC-FTIR microspectroscopy used to screen and detect the co-crystal formation in real time

Tieh-kang Wu, Shan-Yang Lin *, Hong-Liang Lin, Yu-Ting Huang

Department of Biotechnology, Yuanpei University, Hsin-Chu, Taiwan

ARTICLE INFO

Article history:
Received 1 February 2011
Revised 26 February 2011
Accepted 1 March 2011
Available online 4 March 2011

Keywords:
Co-crystal
DSC-FTIR

ABSTRACT

We first report that the formation of pharmaceutical co-crystal can be synchronously screened and confirmed by a simultaneous DSC-FTIR microspectroscopic system, in which this combined unique system giving spectroscopic and thermodynamic information could provide a easy and direct way for one step screening and qualitative detection of the co-crystal formation in real time.

Recently, pharmaceutical co-crystals have gained interesting attention to act as drug candidates in solid-state drug development.[1,2] A pharmaceutical co-crystal, composed of an active pharmaceutical ingredient (API) and a co-former, does not only provide new opportunities to modify the physicochemical properties, dissolution rate, and drug bioavailability of an API, but also creates intellectual property for a new patent of an API for extending their life cycle.[3,4] Thus, the investigations of pharmaceutical co-crystals have been rapidly expanded by growing the number of research publications and patent applications.

Although various methodologies for the preparation of pharmaceutical co-crystals have been employed,[5,6] it might take much time to attempt to prepare the co-crystal formation and then to identify its factuality with different analytical techniques. Therefore, a easy and direct co-crystal screening method is needed in the pharmaceutical industry to improve the screening efficiency in a short time. Until now, there are few techniques available to exactly predict or screen for possible co-crystal formation by a quick procedure.[7,8] To the best of our knowledge, We first report herein a system combining DSC and FTIR to achieve the analysis in one-step. This one-step approach is based on the use of a powerful DSC-FTIR combined microspectroscopic system to simultaneously and directly screen and detect the co-crystal formulation in real time.

Twelve API/co-former combinations were selected for possible screening and detection of co-crystal formation by using this simultaneous DSC-FTIR microspectroscopy. The representative APIs and co-formers were chosen as a demonstration (Scheme 1): indomethacin (IMC) and saccharin (SAC), piroxicam (PIRO) and SAC, or carbamazepine (CBZ) and glutaric acid (GLU). Each pair was homogeneously mixed by the same molar ratio, respectively. A trace amount of the powders mixed was directly pressed within two pieces of KBr pellets by a hydraulic press under 200 kg/cm^2 for 15 s to form a disc. Each sample disc was then determined by a DSC-FTIR microspectroscopic system via a transmission method.[9,10] The raw material of each API or co-former as well as their physical mixture were measured by the conventional DSC and FTIR analysis, respectively. Each solvent-evaporated sample containing API and co-former was also prepared by solvent evaporation. Organic solvents used for preparing each solvent-evaporated sample were acetone for IMC/SAC; chloroform for PIRO/SAC; ethyl acetate for CBZ/GLU, respectively.

The first representative case is studied by using IMC and SAC. The DSC thermograms and FTIR spectra of IMC, SAC, physical mixture and solvent-evaporated sample of IMC/SAC are indicated in Figure 1. Two endothermic peaks at 161 and 229 °C in the DSC curve were attributed to the melting points of IMC (a) and SAC (b), respectively. However, two endothermic peaks at 153 and 183 °C as well as one exothermic peak at 159 °C were observed from the DSC curve of the physical mixture of IMC/SAC (c). The peak appeared at 153 °C might be due to the fusion of eutectic mixture,[7] but the peak at 183 °C was corresponded to the melting point of IMC/SAC co-crystal following the exothermic peak at 159 °C. The solvent-evaporated sample showed an endothermic peak at 183 °C (d), too. The endothermic peak at 183 °C was consistent with the melting point of IMC/SAC co-crystal.[11,12] Due to co-crystal formation between IMC and SAC, a significant IR spectral difference was also found for the physical mixture (c) and solvent-evaporated sample (d) of IMC/SAC. Two unique IR spectral peaks at 1735 and 1682 cm^{-1} were observed for the

* Corresponding author. Tel.: +886 03 5381183x8157; fax: +886 03 6102328.
E-mail address: sylin@mail.ypu.edu.tw (S.-Y. Lin).

0960-894X/$ - see front matter © 2011 Elsevier Ltd. All rights reserved.
doi:10.1016/j.bmcl.2011.03.001

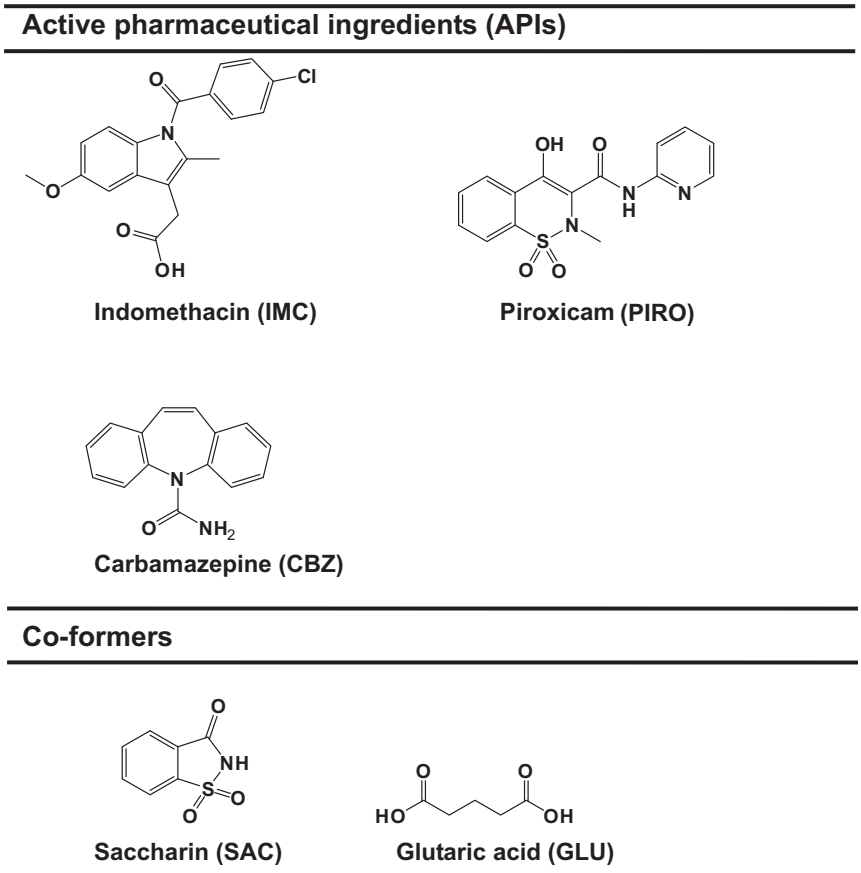

Scheme 1. Chemical structures of the representative APIs and co-formers.

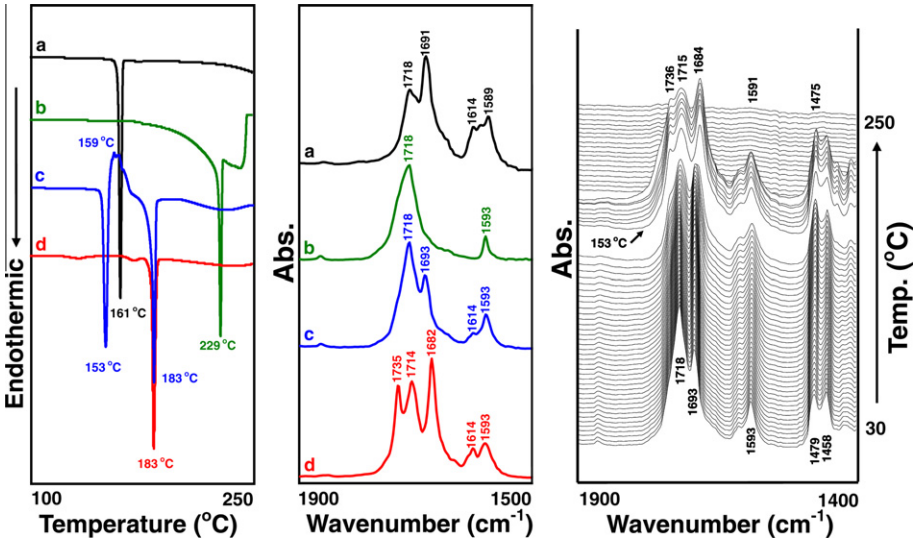

Figure 1. The DSC thermograms and FTIR spectra of IMC (a), SAC (b), physical mixture (c) and solvent-evaporated sample (d) of IMC/SAC, as well as thermal-dependent three-dimensional FTIR spectral plot of the physical mixture of IMC/SAC.

solvent-evaporated sample (d) of IMC/SAC, due to the co-crystal formation occurring via intermolecular hydrogen bonding between IMC and SAC. The thermal-dependent three-dimensional FTIR spectral plot of the physical mixture of IMC/SAC determined by a simultaneous DSC-FTIR microspectroscopy in the IR spectral range within 1900 and 1400 cm^{-1} is also shown in Figure 1. Obviously, before 153 °C the three-dimensional FTIR spectral plot almost maintained the constant contour. Once the temperature was beyond 153 °C, three new IR peaks at 1736, 1718 and 1684 cm^{-1} were observed in the IR spectral map. These three IR peaks at higher temperature almost agreed with the IR spectral data of the solvent-evaporated sample (d), suggesting the actual formation

of IMC/SAC co-crystal. This clearly evidences that the unique and powerful DSC-FTIR microspectroscopic system can easily, directly and simultaneously screen and detect the co-crystal formation of IMC/SAC in real time.

PIRO and SAC are selected for the second study. Figure 2 shows the DSC curves and FTIR spectra of PIRO, SAC, physical mixture and solvent-evaporated sample of PIRO/SAC. Obviously, two sharp endothermic peaks at 202 and 229 °C in the DSC curves were related to the melting point of PIRO (a) and SAC (b), respectively. However, the physical mixture of PIRO/SAC (c) showed a complicated change in the DSC thermogram, in which three endothermic peaks at 167, 196, 221 °C and two exothermic peaks at 169, 198 °C were observed. The appearance of four peaks at 167, 169, 196 and 198 °C will be investigated in the next study, but the peak at 221 °C was the same as the melting point of the solvent-evaporated sample of PIRO/SAC (d). The endothermic peak at 221 °C might be related to the melting point of PIRO/SAC co-crystal,[13,14] suggesting that the co-crystal formation occurred between PIRO and SAC after solvent evaporation. While the IR spectrum of the solvent-evaporated sample of PIRO/SAC (d) was markedly different from that of the physical mixture of PIRO/SAC, in which four specific IR spectral peaks were observed at 1736, 1641, 1607 and 1554 cm^{-1}. The former three IR peaks at 1736, 1641, and 1607 cm^{-1} were found in the three-dimensional FTIR spectral plot (1736, 1639, 1606 cm^{-1}) of the physical mixture of PIRO/SAC determined with a simultaneous DSC-FTIR microspectroscopy. Obviously, the simultaneous DSC-FTIR microspectroscopic system can also directly and immediately screen and detect co-crystal formation of PIRO/SAC in a one-step process, again.

CBZ and GLU are selected in the third study. There are two endotherms (173 and 191 °C) and one exotherm (176 °C) in the DSC curve of CBZ (Fig. 3a). The endothermic peak at 173 °C might be due to the fusion of polymorphic Form III of CBZ,[15,16] while the second endothermic peak at 191 °C was attributed to the melting point of polymorphic Form I of CBZ. The exothermic peak at 176 °C corresponded to the solid–solid polymorphic transition from Form III to Form I of CBZ by recrystallization. GLU (Fig. 3b) also shows a solid–solid transformation near 69–75 °C to a phase with a melting point of 98 °C.[17] While the physical mixture of CBZ/GLU (Fig. 3c) displays three endothermic peaks near 69–75

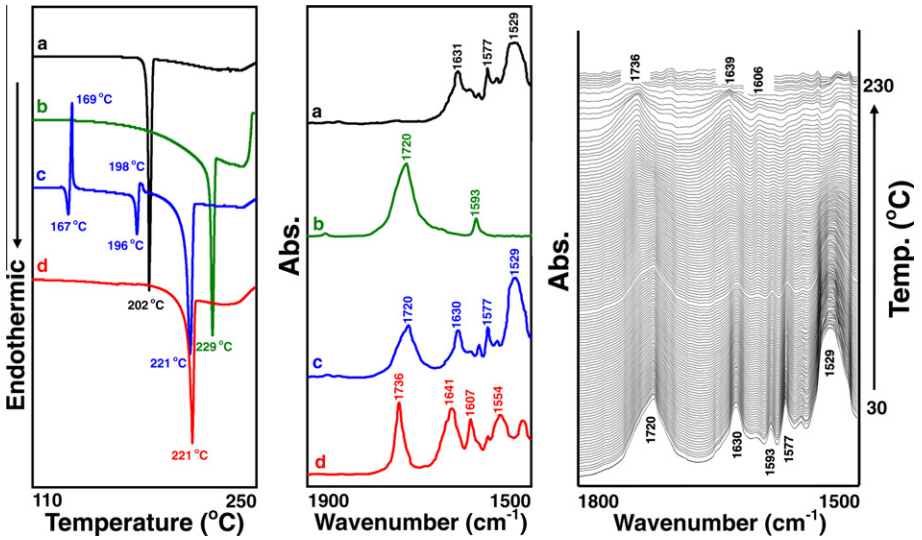

Figure 2. The DSC thermograms and FTIR spectra of PIRO (a), SAC (b), physical mixture (c) and solvent-evaporated sample (d) of PIRO/SAC, as well as thermal-dependent three-dimensional FTIR spectral plot of the physical mixture of PIRO/SAC.

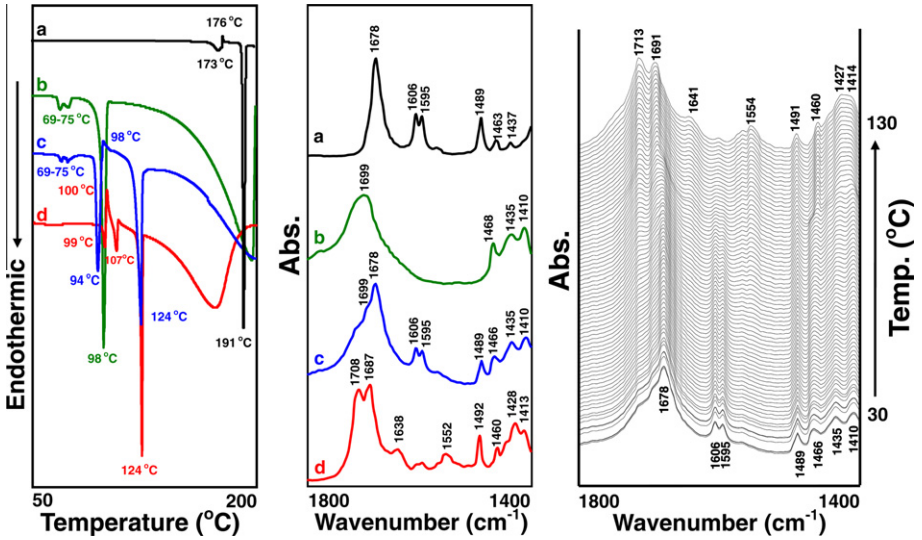

Figure 3. The DSC thermograms and FTIR spectra of CBZ (a), GLU (b), physical mixture (c) and solvent-evaporated sample (d) of CBZ/GLU, as well as thermal-dependent three-dimensional FTIR spectral plot of the physical mixture of CBZ/GLU.

Table 1
The physical mixtures simultaneously screened and detected by using a simultaneous DSC-FTIR microspectroscopy

APIs (mp)[a]	Co-formers (mp)[a]	Co-crystal formed?[b] (mp)[a]	Mp of co-crystal reported[c]
Benzoic acid (122 °C)	Nicotinamide (128 °C)	Yes (91 °C)	
Carbamazepine (191 °C)	Glutaric acid (98 °C)	Yes (124 °C)	125 °C (Ref. 5)
Carbamazepine (191 °C)	Urea (133 °C)	Yes (169 °C)	170 °C[d]
Famotidine (163 °C)	Nicotinamide (128 °C)	No (117 °C)	
Famotidine (163 °C)	Saccharin (226 °C)	No (100–150 °C)	
Indomethacin (162 °C)	Nicotinamide (128 °C)	Yes (127 °C)	123 °C (Ref. 17)
Indomethacin (162 °C)	Saccharin (226 °C)	Yes (183 °C)	183–184 °C (Ref. 3)
Loratadine (135 °C)	Glutaric acid (98 °C)	No (62–95 °C)	
Norfloxacin (221 °C)	Nicotinamide (128 °C)	Yes (188 °C)	
Piroxicam (198 °C)	Saccharin (226 °C)	Yes (221 °C)	222 °C (Ref. 15)
Theophylline (272 °C)	Citric acid (157 °C)	Yes (181 °C)	178 °C (Ref. 19)
Theophylline (272 °C)	Nicotinamide (128 °C)	Yes (172 °C)	174 °C (Ref. 20)

[a] (Mp: melting point) determined by DSC in this study.
[b] Screened and detected by using simultaneous DSC-FTIR microspectroscopy in this study.
[c] Reported from references.
[d] http://www.rsc.org/suppdata/CE/b8/b801713c/b801713c.pdf.

(solid–solid transformation of GLU), 94 (eutectic point of CBZ/GLU) and 124 °C in the DSC thermogram. Beyond 94 °C a co-crystal was formed after an exothermic peak at 98 °C. The peak at 124 °C was the melting point of CBZ/GLU co-crystal, which was consistent with the melting point at 125 °C for the CBZ/GLU co-crystal reported.[5] The solvent-evaporated sample (Fig. 3d) also exhibited an endothermic peak at 124 °C, implying the co-crystal formation after solvent evaporation process.[18] However, two endothermic peaks at 99 and 107 °C and one exothermic peak at 100 °C were observed in the DSC curve of the solvent-evaporated sample before 124 °C, it will be investigated in the future. The FTIR spectrum of the physical mixture of CBZ/GLU (Fig. 3c) was clearly different from that of the IR spectrum of the solvent-evaporated sample of CBZ/GLU (Fig. 3d). Six specific IR peaks at 1708, 1687, 1638, 1552, 1492 and 1428 cm^{-1} were observed from the IR spectrum of the solvent-evaporated sample of CBZ/GLU. These six specific IR peaks were also found in the three-dimensional FTIR spectral profile (1713, 1691, 1641, 1554, 1491, 1427 cm^{-1}) of the physical mixture of CBZ/GLU after measurement with simultaneous DSC-FTIR microspectroscopy. It strongly confirms that the simultaneous DSC-FTIR microspectroscopic system can also effectively provide a one-step screen to determine the CBZ/GLU co-crystal formation in real time.

In this communication, twelve physical mixtures of API and co-former were tested by simultaneous DSC-FTIR microspectroscopy and also confirmed by DSC, as listed in Table 1. Nine co-crystals reported in other studies[5,11–15,17,19,20] were successfully screened and confirmed by a simultaneous DSC-FTIR microspectroscopy using a rapid one-step process. Three physical mixtures that failed to form a co-crystal were also identified by this method. In conclusion, we have extended the use of this unique and powerful technique (DSC-FTIR microspectroscopic system) for synchronous screening and confirming the co-crystal formulation in real time.

Acknowledgements

We wish to thank Misses Yen-Shan Wei and Yung-Fang Chang for their laboratory assistance in this study. This work was supported by National Science Council, Taipei, Taiwan (97-2628-B-264-001-MY3).

References and notes

1. Miroshnyk, I.; Mirza, S.; Sandler, N. *Expert Opin. Drug Delivery* **2009**, *6*, 333.
2. Blagden, N.; Berry, D. J.; Parkin, A.; Javed, H.; Ibrahim, A.; Gavan, P. T.; Luciana, L.; Matos, D.; Seaton, C. C. *New J. Chem.* **2008**, *32*, 1659.
3. Zaworotko, M. *Acta Cryst.* **2008**, *A64*, C11.
4. Trask, A. V. *Mol. Pharm.* **2007**, *4*, 301.
5. Schultheiss, N.; Newman, A. *Cryst. Growth Des.* **2009**, *9*, 2950.
6. Vishweshwar, P.; McMahon, J. A.; Bis, J. A.; Zaworotko, M. J. *J. Pharm. Sci.* **2006**, *95*, 499.
7. Lu, E.; Rodríguez-Hornedo, N.; Suryanarayanan, R. *Cryst. Eng. Commun.* **2008**, *10*, 665.
8. Berry, D. J.; Seaton, C. C.; Clegg, W. R.; Harrington, W.; Coles, S. J.; Norton, P. N.; Hursthouse, M. B.; Storey, R.; Jones, W.; Blagden, N. *Cryst. Growth Des.* **2008**, *8*, 1697.
9. Wang, S. L.; Lin, S. Y.; Chen, T. F.; Chuang, C. H. *J. Pharm. Sci.* **2001**, *90*, 1034.
10. Hsu, C. H.; Ke, W. T.; Lin, S. Y. *J. Pharm. Pharm. Sci.* **2010**, *13*, 67.
11. Padrela, L.; Rodrigues, M. A.; Velaga, S. P.; Matos, H. A.; de Azevedo, E. G. *Eur. J. Pharm. Sci.* **2009**, *38*, 9.
12. Basavoju, S.; Boström, D.; Velaga, S. P. *Pharm. Res.* **2008**, *25*, 530.
13. Bhatt, P. M.; Ravindra, N. V.; Banerjee, R.; Desiraju, G. R. *Chem. Commun.* **2005**, *28*, 1073.
14. Banerjee, R.; Bhatt, P. M.; Ravindra, N. V.; Desiraju, G. R. *Cryst. Growth Des.* **2005**, *5*, 2299.
15. Grzesiak, A. L.; Lang, M.; Kim, K.; Matzger, A. J. *J. Pharm. Sci.* **2003**, *92*, 2260.
16. Rutichelli, C.; Gamberini, G.; Ferioli, V.; Gamberini, M. C.; Ficarra, R.; Tommasini, S. *J. Pharm. Biomed. Anal.* **2000**, *23*, 41.
17. Kojima, T.; Tsutsumi, S.; Yamamoto, K.; Ikeda, Y.; Moriwaki, T. *Int. J. Pharm.* **2010**, *399*, 52.
18. Childs, S. L.; Wood, P. A.; Rodriguez-Hornedo, N.; Reddy, L. S.; Hardcastle, K. I. *Cryst. Growth Des.* **2009**, *9*, 1869.
19. Stevens, J. S.; Byard, S. J.; Schroeder, S. L. M. *Cryst. Growth Des.* **2010**, *10*, 1435.
20. Lu, J.; Rohani, S. *Org. Process. Res. Dev.* **2009**, *13*, 1269.